Performance Analysis of Uplink Index-Modulated NOMA for 6G Wireless Communications

Yoo-Kyung Bae, *Graduate Student Member, IEEE*, Jeong Seon Yeom, *Graduate Student Member, IEEE*, and Bang Chul Jung, *Senior Member, IEEE*

***Abstract*—In this letter, we mathematically analyze the bit-error rate (BER) performance of a *generalized* uplink index-modulated non-orthogonal multiple access (IM-NOMA) system consisting of a base station (BS) with multiple antennas and an arbitrary number of devices with different modulation schemes. We focus on the case that a single subcarrier is activated among $S(\geq 2)$ subcarriers according to index bits to reduce computational complexity. The optimal joint maximum-likelihood (JML) algorithm is assumed to be used for detecting a super-imposed symbol from multiple devices. The closed-form BER is shown to be matched well with simulation results. We also investigate the effect of channel estimation error on the BER. To the best of our knowledge, the mathematical characterization of BER of the generalized uplink IM-NOMA system with an arbitrary number of uplink devices with different modulation schemes and multiple receive antennas at the BS does not exist in the literature. Finally, we show that our analytical framework can be applied to analyze a cell-free massive MIMO NOMA system, which is expected to be one of the most promising techniques for 6G wireless communication systems.**

***Index Terms*—Index modulation (IM), non-orthogonal multiple access (NOMA), bit-error rate (BER), joint maximum-likelihood (JML), imperfect channel state information (CSI).**

I. Introduction

INTERNET of Things (IoT) is considered one of the most emerging techniques for 6G wireless communication systems [1]. With the rapid increase of IoT devices, the frequency shortage in preferred bands is expected to support an enormous amount of uplink data traffic from many IoT devices. In general, the IoT network requires a strict energy efficiency (EE), especially for uplink since most IoT devices are battery-powered [2]. Index modulation (IM) has been actively investigated as an emerging technique to improve both EE and spectral efficiency (SE), where additional information bits are sent by utilizing indices of radio resources like antennas, time slots, and subcarriers. In [3], [4], [5], it was shown that the orthogonal frequency division multiple access (OFDMA) technique with IM improves the EE, error performance, and inter-carrier interference. In [6], a single carrier-frequency division multiple access (SC-FDMA) technique with IM was proposed for uplink narrowband IoT networks to overcome the peak-to-average power ratio (PAPR) problem and improve EE.

On the other hand, a non-orthogonal multiple access (NOMA) technique is expected to be a core radio access technique for future 6G wireless networks [7]. In an uplink NOMA system, multiple devices send signals over the same radio resource simultaneously, and a receiver uses the joint maximum likelihood (JML) detector instead of the successive interference cancellation to provide the optimal error performance [8], [9], [10].

Recently, the index-modulated NOMA (IM-NOMA) technique has been proposed for uplink networks by exploiting the benefits of both IM and NOMA schemes [11], [12], [13]. In [11], the proposed scheme allows multiple transmitters to send additional index bits in a specific timeslot simultaneously and tries to detect multiple transmitters' signals with the JML detector at a *single-antenna* receiver. The upper bound of bit-error rate (BER) performance was also analyzed. In [12], the IM-NOMA technique with various detectors based on SC-FDMA was considered for a *two-user* uplink network and was compared with the conventional NOMA techniques. A suboptimal detection method based on the log-likelihood ratio algorithm was proposed for lower computational complexity than the JML detector [13]. However, the error performance of the uplink IM-NOMA technique has not been thoroughly investigated in a general uplink system which consists of an arbitrary number of uplink devices and an arbitrary number of receive antennas.

In this letter, therefore, we mathematically characterize the BER performance of a *generalized* uplink IM-NOMA system. We assume that L uplink devices send their data over S available subcarriers with the IM simultaneously, and the JML detector is adopted at the base station (BS) with multiple antennas. We assume different modulation schemes of multiple devices and imperfect channel station information (CSI) at the BS. We derive a closed-form BER of the generalized uplink IM-NOMA system, and it is shown that the analysis is matched well with simulation results.

The rest of this letter is organized as follows. In Section II, the system model of the uplink IM-NOMA is described. In Section III, we mathematically analyze the BER performance

Manuscript received 7 March 2023; accepted 26 April 2023. Date of publication 16 May 2023; date of current version 9 August 2023. This work was supported by the Institute for Information and Communications Technology Promotion (IITP) Grant funded by the Korea Government (MSIP, Development of Core Technologies for Unlicensed Band Industrial IoT Network to Overcome Limits of Wireless Connectivity in Manufacturing Factory) under Grant 2020-0-00144. The associate editor coordinating the review of this article and approving it for publication was X. Cheng. (*Yoo-Kyung Bae and Jeong Seon Yeom contributed equally to this work.*) *(Corresponding author: Bang Chul Jung.)*

Yoo-Kyung Bae is with the Land Radar System Team, Hanwha Systems Company Ltd., Yongin 17121, South Korea (e-mail: ykb1103@hanwha.com).

Jeong Seon Yeom and Bang Chul Jung are with the Department of Electronics Engineering, Chungnam National University, Daejeon 34134, South Korea (e-mail: jsyeom@cnu.ac.kr; bcjung@cnu.ac.kr).

Digital Object Identifier 10.1109/LWC.2023.3275944

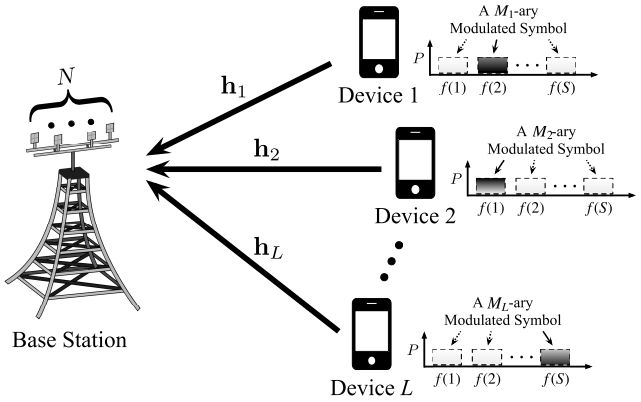

Fig. 1. System model of a generalized uplink IM-NOMA consisting of a BS with multiple antennas and L devices with a single antenna.

by using a union bound and extend the analytical framework to cell-free massive multiple-input multiple output (CF-mMIMO) systems. In Section IV, numerical results are shown in practical system parameters. Finally, conclusions are drawn in Section V.

Notation: Operators on two matrices $\otimes$ and $\circ$ denote the Kronecker and Hadamard products, respectively. $\bar{\mathbf{1}}_{\mathcal{A}}(\cdot)$ denotes a complementary indicator function, i.e., $1-\{\mathbf{1}_{\mathcal{A}}(\cdot)\}$. $\mathrm{diag}(\mathbf{A})$ returns, if $\mathbf{A}$ is a vector, a diagonal matrix whose entries are the elements of vector $\mathbf{A}$, and if $\mathbf{A}$ is a matrix, a column vector containing the diagonal elements of matrix $\mathbf{A}$. $[\mathbf{a}]_i$ denotes i-th element of vector $\mathbf{a}$. $|\mathcal{A}|$ denotes the cardinality of set $\mathcal{A}$.

II. System Model

We consider a generalized uplink IM-NOMA system consisting of a single BS with N antennas and L uplink devices equipped with a single antenna, as shown in Fig. 1. We assume that L devices are located at an arbitrary distance from the BS in a cell, and K subcarriers are activated among S available subcarriers for a general IM operation[1]. Let the l-th ($\in \{1,2,\ldots,L\}$) device send a bit stream (vector), $\mathbf{b}_l$, in each data block. The length of a bit stream $\mathbf{b}$ is denoted as $|\mathbf{b}|$. The bit stream of the l-th device is divided into $\mathbf{b}_{l,\mathrm{sub}}$ and $\mathbf{b}_{l,\mathrm{sym}}$ streams without overlapping, i.e., $|\mathbf{b}_l| = |\mathbf{b}_{l,\mathrm{sub}}| + |\mathbf{b}_{l,\mathrm{sym}}|$. The bit stream $\mathbf{b}_{l,\mathrm{sub}}$, called subcarrier bits or index bits, are used to determine the index of the subcarrier to be activated, and then $|\mathbf{b}_{l,\mathrm{sub}}| = \lfloor \log_2 \binom{S}{K} \rfloor$. The symbol bits, $\mathbf{b}_{l,\mathrm{sym}}$, is used to determine one of M_l-ary phase shift keying (PSK) modulation or M_l-ary quadrature amplitude modulation (QAM) symbol, i.e., $|\mathbf{b}_{l,\mathrm{sym}}| = K\log_2(M_l)$. In this letter, we focus on the case where $K = 1$ for low complexity of both uplink devices and the BS [11]. Then, a received signal vector over S available subcarriers at the BS, $\mathbf{y} \in \mathbb{C}^{SN}$, is given by

$$\mathbf{y} = \sum\nolimits_{l=1}^{L} \sqrt{Pd_l^{-\alpha}}\,\mathrm{diag}(\mathbf{h}_l)\mathbf{x}_l + \mathbf{w} = \mathrm{diag}(\mathbf{G}\mathbf{X}) + \mathbf{w}, \quad (1)$$

[1]Practical wireless systems utilize many subcarriers, e.g., 1024 or 2048. However, we assume that all subcarriers are divided into multiple groups consisting of S subcarriers and focus on a single group with S subcarriers in this letter without loss of generality since all groups operate in the same way.

where P, d_l, and α denote the transmit power of the l-th device, the distance between the BS and the l-th device, and the path-loss exponent, respectively. The transmit power of all uplink devices is assumed to be identical. The wireless channel vector from the l-th device to the BS over S subcarriers is defined as $\mathbf{h}_l \triangleq [\mathbf{h}_l[1]^T \cdots \mathbf{h}_l[S]^T]^T \in \mathbb{C}^{SN}$. Let the estimated channel at the BS be $\hat{\mathbf{h}}_l[n] = \mathbf{h}_l[n] - \boldsymbol{\epsilon}_l[n] \in \mathbb{C}^N$ over the n-th subcarrier, where $\boldsymbol{\epsilon}_l[n]$ denotes the channel estimation error vector that follows independent and identically distributed (i.i.d.) complex normal Gaussian distribution, i.e., $\mathbf{h}_l[n] \sim \mathcal{CN}(\mathbf{0}, \mathbf{I}_N)$ and $\boldsymbol{\epsilon}_l[n] \sim \mathcal{CN}(\mathbf{0}, \sigma_e^2\mathbf{I}_N)$. The transmitted signal of the l-th device is given by $\mathbf{x}_l \triangleq [x_l[1] \cdots x_l[S]]^T \otimes \mathbf{1}_N \in \mathbb{C}^{SN}$, where $x_l[n]$ denotes the transmitted signal of the l-th device over the n-th subcarrier and $\mathbf{1}_N$ indicates an all-ones column vector with length of N. In this letter, a single symbol-modulated signal is sent by using a single subcarrier among S subcarriers since we assume that $K = 1$. The additive white Gaussian noise at the BS is denoted as $\mathbf{w} \sim \mathcal{CN}(\mathbf{0}, N_0\mathbf{I}_{SN})$. The terms of $\mathbf{G}$ and $\mathbf{X}$ are defined as $\mathbf{G} \triangleq [Pd_1^{-\alpha}\mathbf{h}_1 \cdots Pd_L^{-\alpha}\mathbf{h}_L] \in \mathbb{C}^{SN\times L}$ and $\mathbf{X} \triangleq [\mathbf{x}_1, \ldots \mathbf{x}_L]^T \in \mathbb{C}^{L\times SN}$, respectively.

With the optimal JML detector at the BS, the estimates on the transmitted modulation symbols and the active subcarrier from L devices are given by

$$\begin{aligned}(\hat{x}_l, \hat{k}_l)_{l=1}^{L} &= \underset{(s_l,k_l)_{l=1}^{L}\in(\mathcal{X}_l\times\mathcal{K})_{l=1}^{L}}{\arg} \min \left\|\mathbf{y} - \mathrm{diag}\left(\hat{\mathbf{G}}\mathbf{S}\right)\right\|^2 \\ &= \underset{(s_l,k_l)_{l=1}^{L}\in(\mathcal{X}_l\times\mathcal{K})_{l=1}^{L}}{\arg} \min \|\mathbf{y} - \mathrm{diag}(\mathbf{G}\mathbf{S}) + \mathrm{diag}(\mathbf{E}\mathbf{S})\|^2,\end{aligned} \quad (2)$$

where $\hat{x}_l$ and $\hat{k}_l$ denote the estimated modulation symbol and the estimated subcarrier index for the l-th device, respectively. Here, $\mathcal{X}_l$ denotes a set of candidates of modulation symbol of the l-th device and $\mathcal{K} \triangleq \{1,2,\ldots,S\}$. The matrix $\mathbf{S} \triangleq [\mathbf{s}_1,\ldots,\mathbf{s}_L]^T$ consists of the signal candidates, where $\mathbf{s}_l \triangleq s_l\mathbf{e}_{S,k_l} \otimes \mathbf{1}_N$. The term $\mathbf{e}_{S,k_l} \in \mathbb{R}^S$ $(1 \le k_l \le S)$ denotes the standard-basis vector, e.g., $\mathbf{e}_{2,1} = [1\ 0]^T$ and $\mathbf{e}_{2,2} = [0\ 1]^T$ in $\mathbb{R}^2$ for $S = 2$ and $K = 1$. In addition, $\hat{\mathbf{G}} \triangleq [Pd_1^{-\alpha}\hat{\mathbf{h}}_1 \cdots Pd_L^{-\alpha}\hat{\mathbf{h}}_L] \in \mathbb{C}^{SN\times L}$, $\hat{\mathbf{h}}_l \triangleq [\hat{\mathbf{h}}_l[1]^T \cdots \hat{\mathbf{h}}_l[S]^T]^T \in \mathbb{C}^{SN}$ $\mathbf{E} \triangleq [Pd_1^{-\alpha}\boldsymbol{\epsilon}_1 \cdots Pd_L^{-\alpha}\boldsymbol{\epsilon}_L] \in \mathbb{C}^{SN\times L}$, and $\boldsymbol{\epsilon}_l \triangleq [\boldsymbol{\epsilon}_l[1]^T \cdots \boldsymbol{\epsilon}_l[S]^T]^T \in \mathbb{C}^{SN}$.

III. BER Performance Analysis

In this section, we mathematically derive the closed-form BER of the generalized uplink IM-NOMA system. The BER of the l-th device is given by a weighted sum of BERs of symbol bits and (subcarrier) index bit as follows:

$$\Pr(\mathcal{E}_l) = \frac{|\mathbf{b}_{l,\mathrm{sub}}|}{|\mathbf{b}_l|} \times \Pr(\mathcal{E}_{l,\mathrm{sub}}) + \frac{|\mathbf{b}_{l,\mathrm{sym}}|}{|\mathbf{b}_l|} \times \Pr(\mathcal{E}_{l,\mathrm{sym}}), \quad (3)$$

where $\mathcal{E}_{l,\mathrm{sub}}$ and $\mathcal{E}_{l,\mathrm{sym}}$ denote the error event of the symbol and index bits of the l-th device, respectively. As an example, Fig. 2 shows constellation points of all candidates of the received signal in the uplink IM-NOMA system consisting of two devices, where we assume that $N = 1$, $L = 2$, $(S,K) = (2,1)$, and $(M_1,M_2) = (4,4)$ for simplicity. Blue $\times$ marks and solid red circles represent the constellation points of device 1 and device 2, respectively, and the solid green

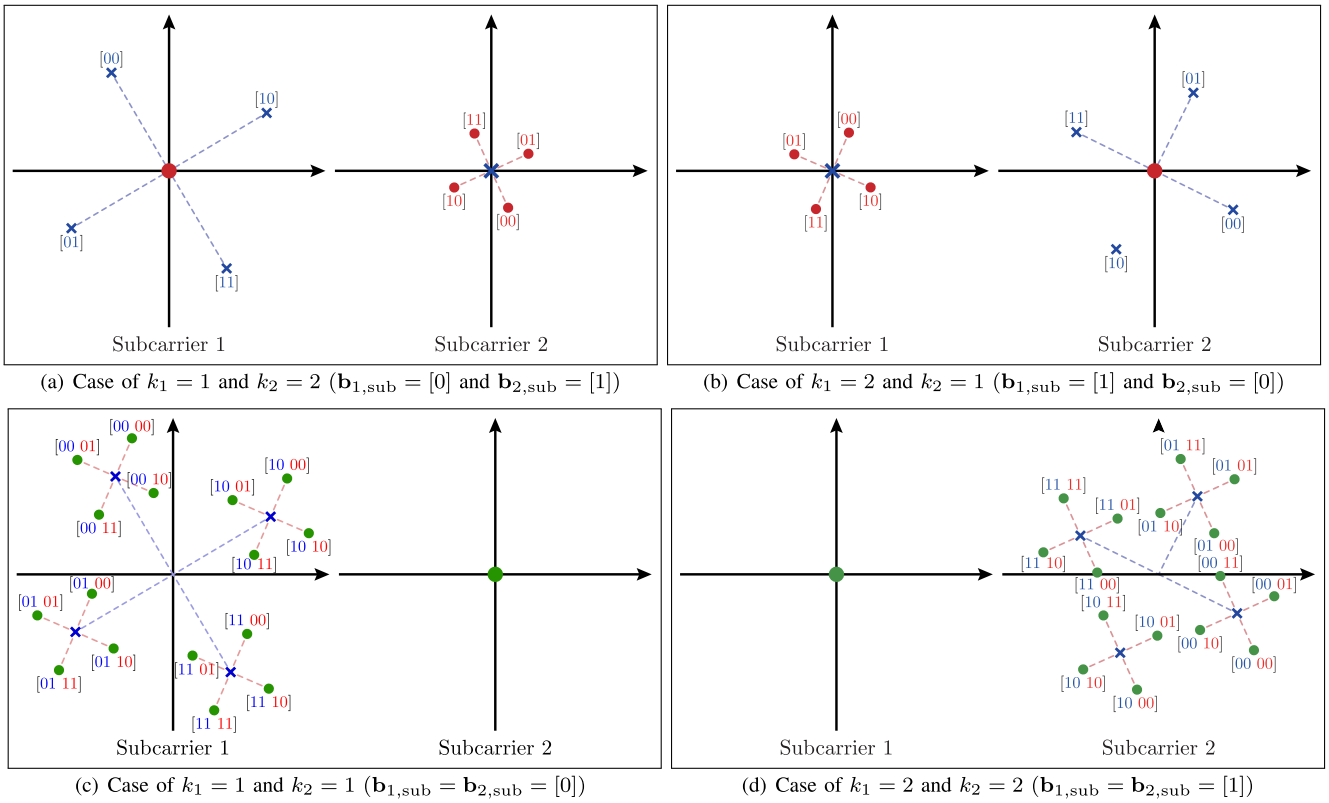

(a) Case of $k_1 = 1$ and $k_2 = 2$ ($\mathbf{b}_{1,\text{sub}} = [0]$ and $\mathbf{b}_{2,\text{sub}} = [1]$)

(b) Case of $k_1 = 2$ and $k_2 = 1$ ($\mathbf{b}_{1,\text{sub}} = [1]$ and $\mathbf{b}_{2,\text{sub}} = [0]$)

(c) Case of $k_1 = 1$ and $k_2 = 1$ ($\mathbf{b}_{1,\text{sub}} = \mathbf{b}_{2,\text{sub}} = [0]$)

(d) Case of $k_1 = 2$ and $k_2 = 2$ ($\mathbf{b}_{1,\text{sub}} = \mathbf{b}_{2,\text{sub}} = [1]$)

Fig. 2. Superimposed QPSK symbols from two devices at the BS when $S = 2$, $K = 1$, and $N = 1$, where $\|\mathbf{h}_1[k]\| > \|\mathbf{h}_2[k]\|$ for all $k \in \{1, 2\}$.

circles indicate constellation points of the superimposed signal when both devices are activated in the same subcarrier. The blue and red bits indicate the symbol bits of device 1 and device 2, respectively. To derive the exact BER, we should obtain the generalized bit error regions in the *SN*-dimensionalconstellation space for all combinations of both index bits and symbol bits, but it is almost impossible. Thus, a conditional BER of the t-th bit of the l-th device for given $\mathbf{G}$ is derived as (4), shown at the bottom of the page, with a union bound, where $\mathcal{S}_{[\mathbf{b}_l]_t=a}$ denotes a set of all signal combinations represented as $\mathbf{S}$ when the t-th bit of the l-th device is equal to $a \in \{0, 1\}$, $\delta[n] \triangleq |[\,\text{diag}(\mathbf{G}(\mathbf{S}_c - \mathbf{S}_e))]_n|$ denotes a Euclidean distance between signal combinations of $\mathbf{S}_c$ and $\mathbf{S}_e$ on the n-th subcarrier. The term $\mathcal{L}_e[n] \subseteq \{1, 2, \ldots, L\}$ denotes a set of indexes of devices whose have a signal on the n-th subcarrier for the symbol matrix $\mathbf{S}_e$. Let $\sigma^2[n] \triangleq 2\sigma_e^2 \sum_{u\in\mathcal{L}_e[n]} Pd_u^{-\alpha}$ and $\gamma[n] \triangleq \frac{|[\sqrt{Pd_1^{-\alpha}} \cdots \sqrt{Pd_L^{-\alpha}}]\cdot([\mathbf{S}_c - \mathbf{S}_e]\cdot\mathbf{e}_{S,n})|^2}{2N_0+\sigma^2[n]}$. Then,

$$\text{diag}\left(\mathbf{G}(\mathbf{S}_c - \mathbf{S}_e)\right) \circ \left([\sqrt{2N_0 + \sigma^2[1]} \cdots \sqrt{2N_0 + \sigma^2[S]}\,]^{-1}\right)^T \sim \mathcal{CN}(\mathbf{0}, \text{diag}([\gamma[1] \cdots \gamma[S]]) \otimes \mathbf{I}_N),$$

since all elements in the channel matrix $\mathbf{G}$ follow i.i.d. complex Gaussian distribution.

Then, the average error probability is derived through expectation of the conditional BER for a given channel matrix with the union bound as shown in (4). If a random variable Z is defined as $Z \triangleq \sum_{n=1}^{S} \delta^2[n]/(2N_0 + \sigma^2[n])$, the union bound of error probability is given by [8]

$$\mathbb{E}\left[Q\left(\sqrt{\sum_{n=1}^{S} \frac{\delta^2[n]}{2N_0 + \sigma^2[n]}}\right)\right] = \int_0^\infty Q\left(\sqrt{z}\right) f_Z(z)\, dz. \quad (5)$$

To represent and generalize the distribution of Z, we first define a scale vector $\boldsymbol{\gamma}^* \in \mathbb{R}^Q$ as a collection of distinct (unique) values of non-zero $\gamma[k]$ for $\forall k$. Then, $\boldsymbol{\gamma}^*$ can be expressed as:

$$[\boldsymbol{\gamma}^*]_q = \begin{cases} \sum_{n=1}^{S} \gamma[n]\left(0^{1-\sum_{k=1}^{n} \bar{\mathbf{1}}_{\{0\}}(\gamma[k])}\right), & \text{for } q = 1 \\ \sum_{n=1}^{S} \gamma[n]\left(0^{1-\sum_{k=1}^{n} \bar{\mathbf{1}}_{\Gamma_q}(\gamma[k])}\right), & \text{for } 2 \le q \le Q, \end{cases}$$

where $\Gamma_q = \{0, [\boldsymbol{\gamma}^*]_1, \ldots, [\boldsymbol{\gamma}^*]_{q-1}\}$. In addition, a shape vector $\boldsymbol{\nu} \in \mathbb{N}^Q$ corresponding to the scale vector is defined as a vector consisting of following elements

$$[\boldsymbol{\nu}]_q = N \times \sum_{u=1}^{S} \mathbf{1}_{\{\gamma[1],\ldots,\gamma[S]\}}([\boldsymbol{\gamma}^*]_q). \quad (6)$$

Then, the distribution of Z is given by

$$Z \sim \text{Hypoexponential}(\boldsymbol{\gamma}^*, \boldsymbol{\nu}), \quad (7)$$

$$\Pr(\mathcal{E}_{l,t}|\mathbf{G}) \le \frac{1}{2} \sum_{a=0}^{1} \frac{1}{|\mathcal{S}_{[\mathbf{b}_l]_t=a}|} \sum_{\mathbf{S}_c \in \mathcal{S}_{[\mathbf{b}_l]_t=a}} \sum_{\mathbf{S}_e \in \mathcal{S}_{[\mathbf{b}_l]_t \neq a}} Q\left(\sqrt{\sum_{n=1}^{S} \frac{\delta^2[n]/2}{N_0 + \sigma_e^2 \sum_{u\in\mathcal{L}_e[n]} Pd_u^{-\alpha}}}\right) \quad (4)$$

and $f_Z(z)$ is given by [14]:

$$f_Z(z) = \sum_{i=1}^{|\boldsymbol{\gamma}^*|} \sum_{j=1}^{[\boldsymbol{\nu}]_i} A_{i,j} \frac{z^{j-1}}{(j-1)!([\boldsymbol{\gamma}^*]_i)^j} e^{-\frac{z}{[\boldsymbol{\gamma}^*]_i}}, \quad (8)$$

where $A_{i,j}$ is derived as a solution of a linear matrix equation of the Kad matrix [14].

By substituting (8) into (5), we obtain the BER of t-th bit of the l-th device of the uplink IM-NOMA system with multiple receiver antennas as follows:

$$\Pr\{\mathcal{E}_{l,t}\} \le \frac{1}{2} \sum_{a=0}^{1} \frac{1}{|\mathcal{S}_{[\mathbf{b}_l]_t=a}|} \sum_{\mathbf{s}_c \in \mathcal{S}_{[\mathbf{b}_l]_t=a}} \sum_{\mathbf{s}_e \in \mathcal{S}_{[\mathbf{b}_l]_t \neq a}} \times \left[\sum_{i=1}^{|\boldsymbol{\gamma}^*|} \sum_{j=1}^{[\boldsymbol{\nu}]_i} \frac{A_{i,j}}{2} \left\{ 1 - \sum_{k=0}^{j-1} \binom{2k}{k} \sqrt{\frac{1}{1+2/[\boldsymbol{\gamma}^*]_i}} \frac{1}{(4+2[\boldsymbol{\gamma}^*]_i)^k} \right\} \right]. \quad (9)$$

We now explain that our mathematical framework to analyze the uplink IM-NOMA system is still valid when analyzing BER performance of the NOMA system in CF-mMIMO networks [15]. The basic concept of the uplink CF-mMIMO is for multiple distributed BSs (or equivalently radio units, RUs) to cooperatively receive signals from devices and convey the received signals to a central processing unit (CPU) through wired or wireless backhaul links [15]. Then, the CPU decodes the information of devices by synthesizing the signals from multiple BSs.

Assuming that the r-th ($r \in \{1, 2, \ldots, R\}$) BS is equipped with N_r antennas, each BS (or RUs) handles SN_r-dimensional complex valued signals. The square of error distance, δ_s^2 becomes a random variable following Erlang distribution with N_r shape and γ_s^2 scale for N_r-dimensional complex valued signals over the s-th subcairrer. Then, sum of the square of S error distances follows the hypoexponential distribution as well. Similarly, the CPU of CF-mMIMO system handles $(\sum_{r=1}^{R} N_r)$-dimensional complex valued signals and the square of error distance, δ_r^2. The element of N_r-dimensional complex valued signals of the r-th BS becomes a random variable following Erlang distribution with N_r shape and γ_r^2 scale. Finally, the sum of square of R error distances follows the hypoexponential distribution. As a result, (9) can be applied to BER analysis of the uplink NOMA system in CF-mMIMO networks by regarding subcarrier-related variables of the uplink IM-NOMA system as receive antenna-related variables in the uplink NOMA system in CF-mMIMO networks.

IV. Simulation Results

In this section, we validate the BER performance of the uplink IM-NOMA system through computer simulations.

Fig. 3 shows the average BER of the uplink IM-NOMA system with the JML detector for varying the transmit SNR when $L = 2$, $(S, K) = (2, 1)$, $N = 4$, $M_1 = M_2 = 4$, and $(d_1, d_2) = (2, 1)$. In this case, $(|\mathbf{b}_{l,\text{sub}}|, |\mathbf{b}_{l,\text{sym}}|) = (1, 2)$. Analysis results are matched well with computer simulation results as the SNR increases. In this figure, we compare the uplink IM-NOMA with NOMA in terms of BER. For fair comparion, two devices in the conventional uplink NOMA system transmit QPSK and BPSK signals over two subcarriers, respectively. Then, $M_l \triangleq (M_l[1], M_l[2])$ denotes the used

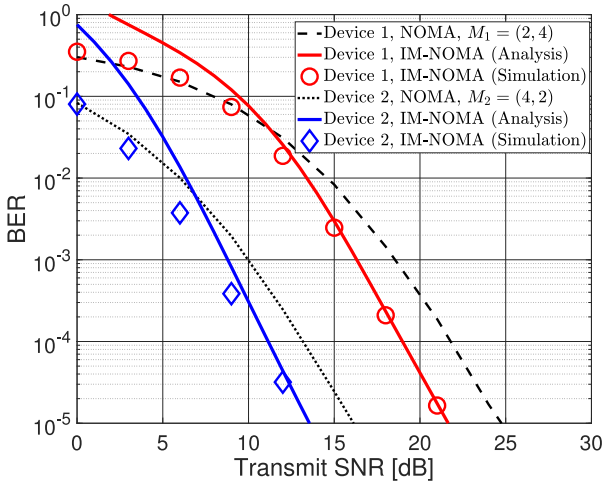

Fig. 3. BER of uplink IM-NOMA and conventional uplink NOMA systems when $L = 2$, $S = 2$, $N = 4$, $|\mathbf{b}_l| = 3$, $(d_1, d_2) = (2, 1)$, and $\sigma_e^2 = 0$.

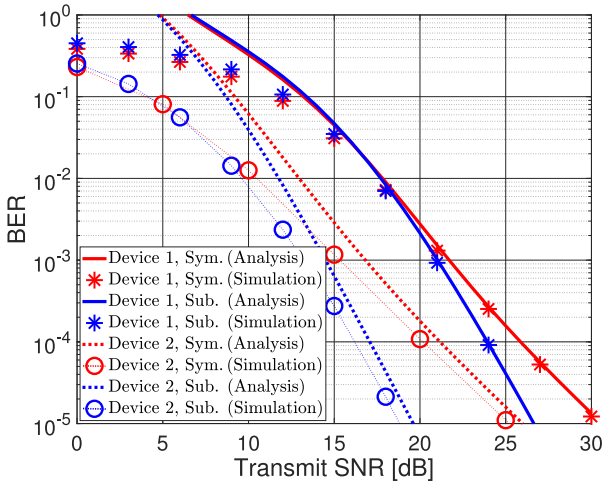

Fig. 4. BER comparison of index and symbol bits in the uplink IM-NOMA system when $L = 2$, $N = 2$, $(S, K) = (4, 1)$, $(M_1, M_2) = (2, 4)$, $(d_1, d_2) = (2, 1)$, and $\sigma_e^2 = 0$.

modulation orders of the l-th device for two subcarriers in the conventional NOMA system. The total power for both the conventional NOMA and the IM-NOMA is set to be the same. Note that the BER performance of the IM-NOMA becomes better than that of the conventional NOMA when the SNR is high.

Fig. 4 compares BERs of index bits and symbol bits in the uplink IM-NOMA system when $L = 2$, $(S, K) = (4, 1)$, $N = 2$, $(M_1, M_2) = (2, 4)$, $(d_1, d_2) = (2, 1)$, and $\sigma_e^2 = 0$. Somewhat interestingly, the BER performance of index bits is better than that of symbol bits. Especially in high SNRs, the slopes of BER become different from each other. Fig. 5 shows the BER performance of the uplink IM-NOMA system with imperfect CSI, $\sigma_e^2 = 0.01$, when $L = 3$, $(S, K) = (4, 1)$, $N = 2$, $(M_1, M_2, M_3) = (4, 2, 2)$, and $(d_1, d_2, d_3) = (2, 1.5, 1)$. We verify that the analytical framework proposed in this letter works well even with imperfect CSI environments.

Fig. 6 shows a normalized effective throughput for varying number of available subcarriers S when $L = 2$, $N = 4$,

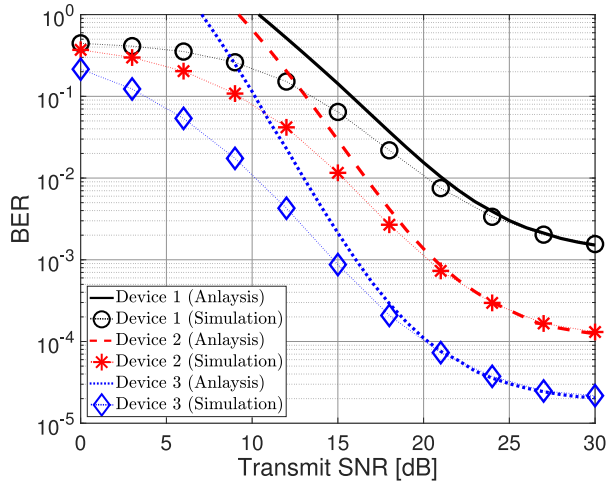

Fig. 5. BER of the uplink IM-NOMA system with imperfect CSI when $L = 3$, $(S, K) = (4, 1)$, $N = 2$, $(M_1, M_2, M_3) = (4, 2, 2)$, $(d_1, d_2, d_3) = (2, 1.5, 1)$, and $\sigma_e^2 = 0.01$.

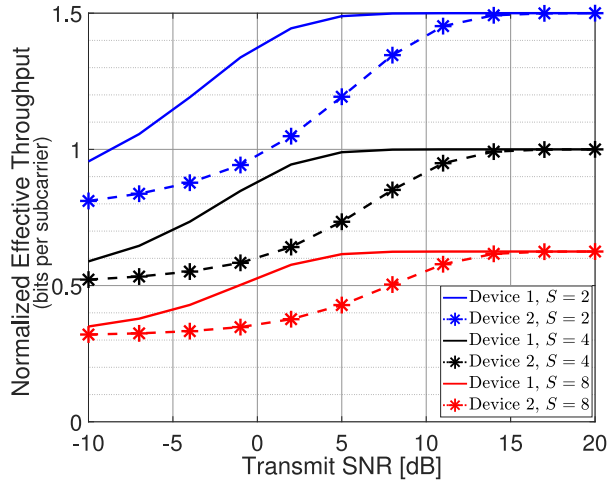

Fig. 6. Normalized effective throughput of the uplink IM-NOMA system with the JML detector for a various number of available subcarriers $S = 2$, 4 and 8 when $L = 2$, $N = 4$, $M = 4$, $K = 1$, and $(d_1, d_2) = (1, 2)$.

$M = 4$, $K = 1$, and $(d_1, d_2) = (1, 2)$. The effective spectral efficiency (Effective SE) is defined as $(|\mathbf{b}_{l,\mathrm{sym}}| + |\mathbf{b}_{l,\mathrm{sub}}|)/S$. The *normalized effective throughput* [16] of the l-th device $(l \in \{1, 2\})$ is given by

$$\mathsf{NET}_l = \mathsf{Effective\ SE} \times (1 - \Pr(\mathcal{E}_l)). \tag{10}$$

As the number of available subcarriers S increases, the number of bits embedded through the IM $|\mathbf{b}_{l,\mathrm{sub}}|$ increases but the effective SE decreases. For example, if S is equal to 2, 4, and 8, then its corresponding effective SE becomes equal to 1.5, 1, and 0.625, respectively. From Fig. 6, we observe that the normalized effective throughput increases as the number of available subcarriers decreases in the uplink IM-NOMA system with the JML detector. This comes from the fact that the effective throughput becomes increased as S becomes decreased, while the BER performances remain similar even though the number of available subcarriers are different.

Through additional simulations, we can confirm that the degradation of BER performance is small at the expense of complexity of the JML detection even when the number of devices increases further. These results are omitted due to lack of quantity.

V. Conclusion

We mathematically analyzed the bit-error rate (BER) performance of a generalized uplink index modulated non-orthogonal multiple access (IM-NOMA) system under perfect and imperfect channel state information, where the joint maximum-likelihood (JML) detector is adopted at the base station (BS) equipped with multiple antennas for decoding signals from an arbitrary number of devices. We assume an arbitrary number of available subcarriers and different modulation schemes at devices. Through computer simulations, it was shown that the analytical results are matched well with the simulation results especially as the signal-to-noise ratio increases. Furthermore, we validated the uplink IM-NOMA technique via extensive computer simulations in terms of error performance and normalized effective throughput.

References

[1] D. C. Nguyen et al., "6G Internet of Things: A comprehensive survey," *IEEE Internet Things J.*, vol. 9, no. 1, pp. 359–383, Jan. 2022.
[2] A. H. M. Aman, E. Yadegaridehkordi, Z. S. Attarbashi, R. Hassan, and Y.-J. Park, "A survey on trend and classification of Internet of Things reviews," *IEEE Access*, vol. 8, pp. 111763–111782, 2020.
[3] E. Başar, Ü. Aygölü, E. Panayırcı, and H. V. Poor, "Orthogonal frequency division multiplexing with index modulation," *IEEE Trans. Signal Process.*, vol. 61, no. 22, pp. 5536–5549, Nov. 2013.
[4] L. Xiao, B. Xu, H. Bai, Y. Xiao, X. Lei, and S. Li, "Performance evaluation in PAPR and ICI for ISIM-OFDM systems," in *Proc. Int. Workshop High Mobility Wireless Commun.*, Nov. 2014, pp. 84–88.
[5] A. Tusha, S. Doğan, and H. Arslan, "A hybrid downlink NOMA with OFDM and OFDM-IM for beyond 5G wireless networks," *IEEE Signal Process. Lett.*, vol. 27, pp. 491–495, Mar. 2020.
[6] J. Manco-Vasquez, M. Chafii, and F. Bader, "Tailoring index-modulation for uplink IoT and M2M networks," in *Proc. IEEE Wireless Commun. Netw. Conf. (WCNC)*, Apr. 2019, pp. 1–6.
[7] Y. Liu et al., "Evolution of NOMA toward next generation multiple access (NGMA) for 6G," *IEEE J. Sel. Areas Commun.*, vol. 40, no. 4, pp. 1037–1071, Apr. 2022.
[8] J. S. Yeom, H. S. Jang, K. S. Ko, and B. C. Jung, "BER performance of uplink NOMA with joint maximum-likelihood detector," *IEEE Trans. Veh. Technol.*, vol. 68, no. 10, pp. 10295–10300, Oct. 2019.
[9] H. Semira, F. Kara, H. Kaya, and H. Yanikomeroglu, "Multi-user joint maximum-likelihood detection in uplink NOMA-IoT networks: Removing the error floor," *IEEE Wireless Commun. Lett.*, vol. 10, no. 11, pp. 2459–2463, Nov. 2021.
[10] K.-H. Lee, J. S. Yeom, J. Joung, and B. C. Jung, "Performance analysis of uplink NOMA with constellation–rotated STLC for IoT networks," *IEEE Open J. Commun. Soc.*, vol. 3, pp. 705–717, 2022.
[11] S. Althunibat, R. Mesleh, and T. F. Rahman, "A novel uplink multiple access technique based on index-modulation concept," *IEEE Trans. Commun.*, vol. 67, no. 7, pp. 4848–4855, Jul. 2019.
[12] M. B. Shahab, S. J. Johnson, M. Shirvanimoghaddam, M. Chafii, E. Basar, and M. Dohler, "Index modulation aided uplink NOMA for massive machine type communications," *IEEE Wireless Commun. Lett.*, vol. 9, no. 12, pp. 2159–2162, Dec. 2020.
[13] J. Li, Q. Li, S. Dang, M. Wen, X.-Q. Jiang, and Y. Peng, "Low-complexity detection for index modulation multiple access," *IEEE Wireless Commun. Lett.*, vol. 9, no. 7, pp. 943–947, Jul. 2020.
[14] K. Smaili, T. Kadri, and S. Kadry, "Finding the PDF of the hypoexponential random variable using the Kad matrix similar to the general Vandermonde matrix," *Commun. Stat. Theory Methods*, vol. 45, no. 5, pp. 1542–1549, Feb. 2016.
[15] S. Elhoushy, M. Ibrahim, and W. Hamouda, "Cell-free massive MIMO: A survey," *IEEE Commun. Surveys Tuts.*, vol. 24, no. 1, pp. 492–523, 1st Quart., 2022.
[16] D. Shen, Z. Pan, K.-K. Wong, and V. Li, "Effective throughput: A unified benchmark for pilot-aided OFDM/SDMA wireless communication systems," in *Proc. 22nd Joint Conf. IEEE Comput. Commun. Soc. (INFOCOM)*, Mar. 2003, pp. 1603–1613.